

An AFC (assimilation and fractional crystallization) process as the petrogenesis of andesites from the Pliocene Myojin-iwa Formation, the back-arc side of the Northeast Japan: combined major- and trace-element and Sr-Nd isotope constraints

Abstract

*Hiromi Kondo**, *Kenji Shuto*** and *Masayuki Fukase**** Andesitic rocks, of the Pliocene Myojin-iwa volcanic field, in the northern part of Niigata Prefecture, Northeast Japan, show transitional chemical characteristics between typical calc-alkaline and tholeiitic series. The most primitive basaltic andesite among these andesitic rocks (the Myojin-iwa Formation) has geochemical characteristics similar to those of other Pliocene-Quaternary basaltic rocks from the back-arc side of the NE Japan, and has initial Sr isotope ratio slightly higher than those of the latter basaltic rocks.

Received June 17, 1999.

Accepted January 19, 2000.

* Hosei University Daini High School, Kiduki oomati 164, Nakahara-ku, Kawasaki 211-0031, Japan

** Department of Geology, Faculty of Science, Niigata University, Ikarashi 2-machi 8050, Niigata 950-2181, Japan

*** Graduate School of Science and Technology, Niigata University, Ikarashi 2-machi 8050, Niigata 950-2181, Japan

Andesites from the Myojin-iwa area show SiO₂ contents ranging from 53.3% to 62.8, and initial Sr and Nd isotope ratios vary from 0.70324 to 0.70378 and 0.512791 to 0.512926, respectively. The initial Sr isotope ratios display positive correlation with SiO₂, and their initial Nd isotope ratios gradually decrease with increasing SiO₂. This suggests that the genesis of andesites from the area can not be attributed to simple fractional crystallization of the primary basaltic magma, but to an assimilation and fractional crystallization (AFC) process. Based on petrographical evidence, major and trace element compositions and Sr-Nd isotope systematics, the Paleogene granitoid rocks constituting the upper crust beneath the Myojin-iwa and surrounding areas are the possible candidates for assimilants. An AFC model using the granitoid rocks as the assimilant can successfully reproduce the chemical variations of the andesites from the Myojin-iwa Formation by assuming the *r* values (ratio of the rate of assimilation to the rate of fractional crystallization) of less than 0.2.

Key words: back-arc volcanism, Northeast Japan, Pliocene, andesite, Sr and Nd isotopes, AFC process

Introduction

The origin of calc-alkaline andesites remains one of the most important problems in island-arc igneous petrogenesis. Since the 1970's, the importance of magma mixing in the evolution of the calc-alkaline andesite magma has been emphasized (e.g., Eichelberger, 1975; Anderson, 1976; Sakuyama, 1981), and the mechanism for magma mixing has been studied in detail (e.g., Koyaguchi and Blake, 1989; Takada, 1994), while, in recent years, high quality analyses of

trace elements and radiogenic and stable isotopes have been shown to be a powerful tool for identifying the role of crustal assimilation in the petrogenesis of volcanic rocks (e.g., James, 1982; Petrini et al., 1987). Accordingly, it may be significant to evaluate the effects of crustal assimilation in addition to those of magma mixing when examining the evolutionary process of calc-alkaline igneous rocks.

Chemically transitional andesitic rocks, between typical calc-alkaline and tholeiitic series, occur in the Pliocene Myojin-iwa Andesite Formation (Takahama,

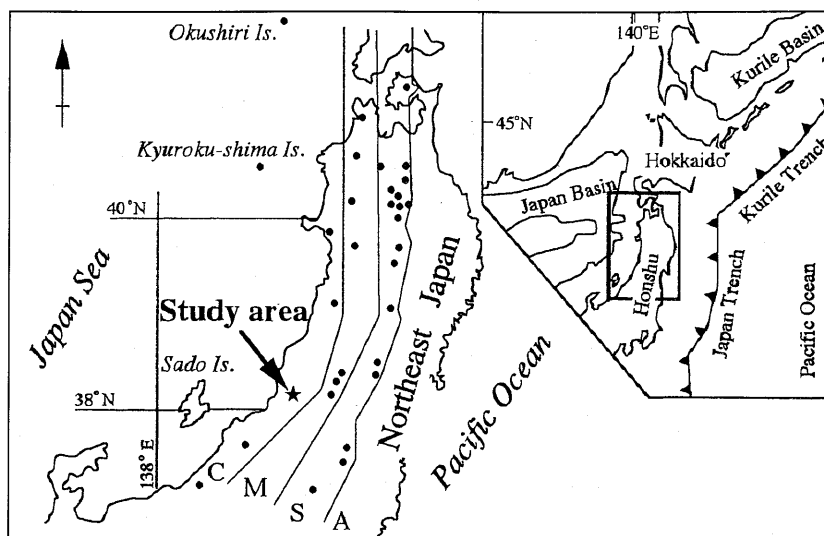


Fig. 1. Index map showing the study area and distribution of the Pliocene volcanic rocks (solid circles) in the NE Japan (after Shuto and Yashima, 1990). Solid lines show the boundaries of the Quaternary volcanic zones, Aoso-Osore (A), Sekiryu (S), Moriyoshi (M) and Chokai (C) zones after Nakagawa et al. (1986).

1976) in the northern part of Niigata Prefecture, NE Japan. This paper uses the name “the Myojin-iwa Formation” instead of “the Myojin-iwa Andesite Formation”: it describes the petrographic and geochemical characteristics of these andesitic rocks. Based on the petrographic and geochemical data, we discuss a crustal assimilation and fractional crystallization (AFC) model as a plausible process to cause the compositional variations of these andesitic rocks.

Geological setting

The NE Japan is situated on the convergent plate boundary between the Eurasian and Pacific plates, and has the characteristics of a typical arc-trench system. Quaternary volcanic rocks are distributed in a zone 100~150 km wide extending from central Honshu to southwestern Hokkaido (Fig. 1). A gradual increase in alkali contents, especially in K₂O, other large ion lithophile elements (LIL elements), and high field strength elements (HFS elements) from the Pacific Ocean side (the trench side) to the Japan Sea side (the back-arc side) across the NE Japan is well documented (e.g., Kuno, 1960; Kawano et al., 1961; Masuda, 1979; Yoshida and Aoki, 1984; Fujimaki and Kurasawa, 1980; Sakuyama and Nesbitt, 1986; Nakagawa et al., 1988).

Volcanic rocks in Pliocene age (4 to 2 Ma) show similar distribution (Fig. 1) and geochemical zonation to those of Quaternary volcanic rocks (Fukudome et al., 1990; Shuto and Yashima, 1990; Nakajima et al., 1995). On the back-arc side of the NE Japan, small-scale Pliocene volcanic bodies occur in scattered exposures, mostly as lavas and pyroclastic rocks which are composed mainly of calc-alkaline andesites and dacites with minor amounts of alkaline basaltic rocks (Fukudome et al., 1990; Shuto and Yashima, 1990;

Nakajima et al., 1995). Detailed petrological investigations of these volcanic bodies have not previously been undertaken: they may provide geochemical data useful to the discussion of the genesis of the island arc andesitic rocks.

Stratigraphy

The study area is located in the northern part of Niigata Prefecture (called here the Niigata area), about 10 km inland from the Japan Sea coast (Fig. 1), where the Myojin-iwa Formation unconformably overlies middle Miocene sedimentary rocks composed mainly of black shale. The Myojin-iwa Formation also occurs in faulted contact with early Miocene volcanic rocks composed mainly of altered andesitic pyroclastic rocks in the western part of the study area (Fig. 2).

The formation is exposed over an area of 3 km (N-S) × 4 km (E-W). Lithologically it can be divided into three units; the lower, middle and upper units. The lower unit consists mainly of andesitic pyroclastic rocks including tuff breccia and volcanic breccia, associated with minor amounts of dark gray to black lavas which are intercalated with thin beds of rhyolitic pumiceous tuff and sandstone. The total thickness of this unit ranges from 300 to 350 m. In contrast, the middle unit consists of numerous dark gray to black andesitic lavas ranging in thickness from 10 to 50 m, which are frequently intercalated with pyroclastic rocks. Continuous outcrops of massive and autobrecciated lavas with frequent intercalations of lappili tuff, tuff breccia and volcanic breccia of this unit, crop-out along the Kogoyasawa River. This unit is more than 300 m thick and conformably overlies the lower unit. The upper unit consists of pyroclastic rocks, including tuff breccia and lappili

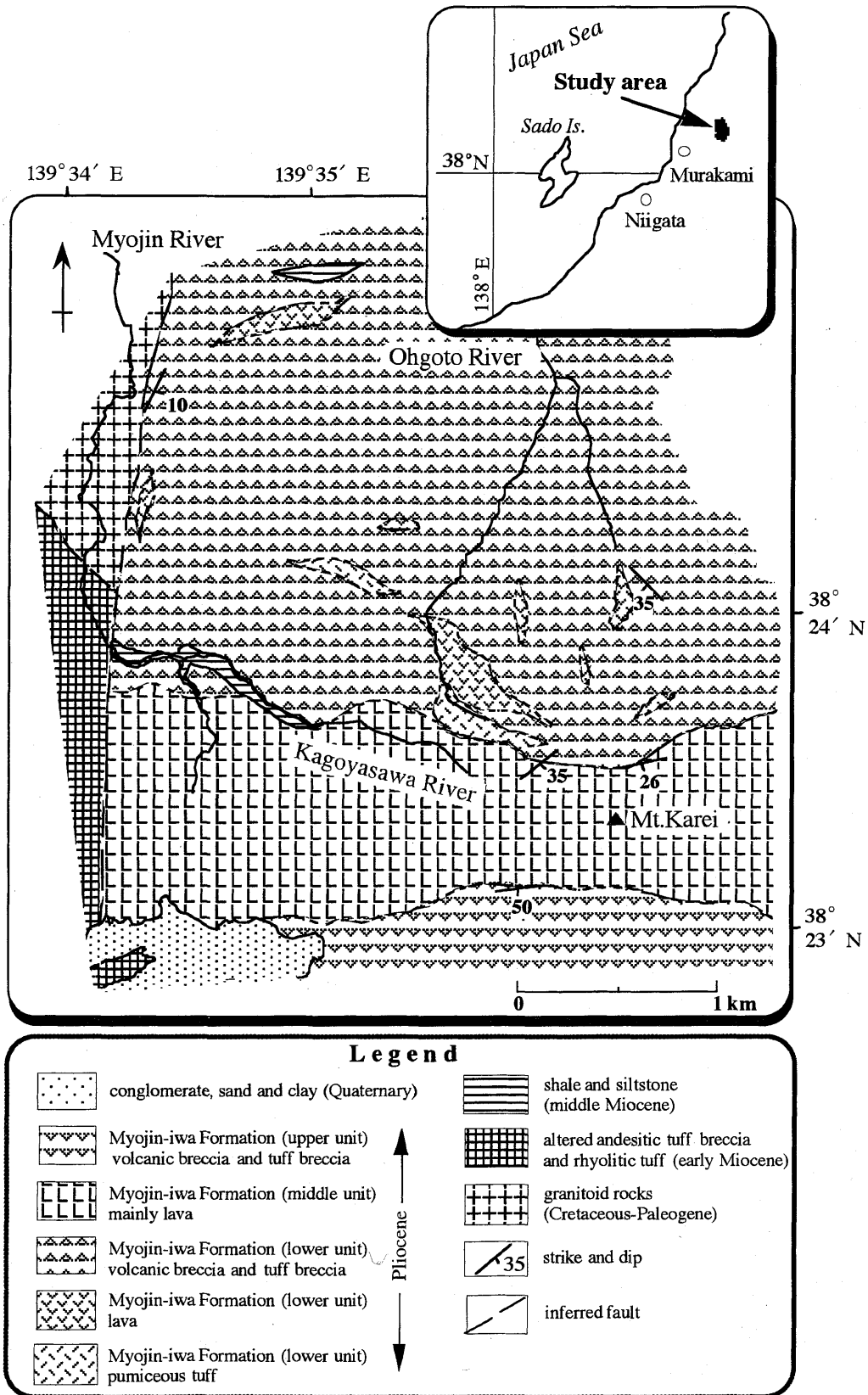


Fig. 2. Geologic map of the Myojin-iwa area. Location is shown in Fig. 1.

Table 1. Modal compositions of volcanic rocks from the study area.

Sample No.	L141	L138	L123	L105	M5	M6	M150	M157	M354	M191
Phenocryst	41.7	42.9	36.1	30.8	45.4	32.8	41.3	36.4	45.8	43.9
Ol	-	-	-	-	2.6	-	-	-	-	-
Cpx	6.8	7.8	5.2	4.3	14.5	5.3	8.3	1.8	6.5	3.6
Opx	2.8	2.5	1.5	2.5	6.9	1.5	4.3	1.2	3.8	5.4
Hb	-	-	-	-	-	-	-	-	-	-
Fe-Ti oxide	-	0.8	1.1	3.5	-	1.1	0.9	1.5	4.3	3.8
Pl	32.1	31.8	28.3	20.5	21.4	24.9	27.8	31.9	31.2	31.1
Groundmass	58.3	57.1	63.9	69.2	54.6	67.2	58.7	63.6	54.2	56.1
Sample No.	M202	M7	M33	M32	M91	M4	M154	M63	M1	M95
Phenocryst	29.5	42.1	25.1	24.1	36.1	43.3	52.7	36.4	28.6	36.2
Ol	-	-	-	-	-	-	-	-	-	-
Cpx	4.4	6.5	3.7	1.2	4.2	4.1	3.1	4.7	1.7	-
Opx	5.3	4.5	0.6	3.5	3.5	3.1	7.7	1.1	0.5	0.8
Hb	-	-	-	-	-	0.2	0.2	0.1	4.2	2.7
Fe-Ti oxide	1.9	2.1	1.7	1.2	1.9	2.8	8.5	1.4	1.3	2.4
Pl	17.9	29.0	19.1	18.2	26.5	33.1	33.2	29.1	20.9	30.3
Groundmass	70.5	57.9	74.9	75.9	63.9	56.7	47.3	63.6	71.4	63.8

Ol; olivine, Cpx; clinopyroxene, Opx; orthopyroxene, Hb; hornblende, Pl; plagioclase, L141-L105; rocks of the lower unit, M5-M95; rocks of the middle unit

tuff with fragments of andesite in matrix of dark gray andesitic tuff. This unit has the thickness more than 100m and conformably overlies the middle unit.

One andesite sample from the lower unit gave a K-Ar age of 3.1 Ma (Agency of Natural Resources and Energy, 1982). Considering the gradational stratigraphic relationships between the three units and the similarities in the lithofacies of lavas and pyroclastic rocks from the three units, these andesitic rocks were derived from a volcano which was active for a relatively short period of about 3 Ma.

Petrography and mineral chemistry

The andesites of the Myojin-iwa Formation, mainly lavas from the lower and middle units, can be divided into four types on the basis of their mineral assemblages: 1) olivine-pyroxene basaltic andesite, 2) pyroxene basaltic andesite and pyroxene andesite, 3) hornblende-bearing pyroxene andesite, and 4) pyroxene-hornblende andesite. The modal compositions of the representative andesitic rocks are shown in Table 1.

1. olivine-pyroxene basaltic andesite

This type (sample M5) occurs as a lava from the middle unit. It is porphyritic with 45.4 vol% phenocrysts of plagioclase (21.4%), clinopyroxene (14.5%), orthopyroxene (6.9%), olivine (2.6%) and a minor amount of Fe-Ti oxide. Plagioclase phenocrysts, which are 0.5-3mm long, are generally fresh. Clinopyroxene (0.5-3mm long) and orthopyroxene (0.5-2mm long) phenocrysts are also fresh and frequently form glomeroporphyritic aggregates with plagioclase. All grains of phenocrystic olivine (0.5-

0.8mm long) are altered to calcite and clay minerals. Fe-Ti oxides (less than 0.3mm long) are sporadically found. The groundmass is intergranular, and consists of plagioclase, clinopyroxene, orthopyroxene, Fe-Ti oxides and brown glass.

Plagioclase phenocryst core compositions in this sample fall within a relatively narrow compositional variation range between An=65 and An=91 (Fig. 3). Although normal zoning is the most common type among phenocryst plagioclases, some reversally zoned plagioclase grains cooccur. Clino- and orthopyroxene phenocrysts have restricted core compositions (Mg-values=74-84 for clinopyroxene and 68-73 for orthopyroxene) (Fig. 4). These pyroxenes display weak normal zoning in terms of Mg-value.

2. pyroxene basaltic andesite and pyroxene andesite

This rock type is the most common constituent of the Myojin-iwa Formation. The basaltic andesite and andesite are porphyritic, containing 24.1-45.8 vol % phenocrysts of plagioclase (17.9-32.1%), clinopyroxene (1.2-8.3 %), orthopyroxene (0.6-5.4 %) and Fe-Ti oxides (0.8-4.3 %). These minerals usually show euhedral to subhedral form that is found not only as discrete phenocrysts, but also as glomeroporphyritic aggregates of 2-4 mm in diameter.

Plagioclase phenocrysts, which are 0.5-3.3 mm long, are generally fresh, but some have dusy zones. Clinopyroxene (0.5-2 mm long) and orthopyroxene (0.5-2mm long) phenocrysts are mostly fresh, but some orthopyroxenes are altered to calcite. Fe-Ti oxide phenocrysts (less than 0.5 mm across) are mostly titanomagnetite. The rocks with SiO₂ contents lower

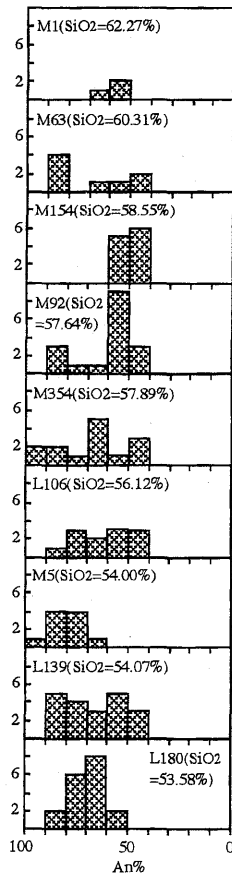


Fig. 3. Frequency of An % in the cores of plagioclase phenocrysts in the andesites from the Myojin-iwa Formation. SiO₂ contents are those of whole rocks.

than about 58% show mostly intersertal or intergranular texture consisting mainly of plagioclase, clinopyroxene, orthopyroxene, Fe-Ti oxides and glass, whereas rocks with SiO₂ contents greater than 58% show mostly hyalopilitic or hyalo-ophitic texture consisting of plagioclase microlite, Fe-Ti oxides and glass.

The plagioclase phenocryst cores in five samples show a relatively wide compositional range (An=44–87 for L 106, 43–89 for L 139, 51–90 for M 180, 46–84 for M 92 and 47–84 for M 354) (Fig. 3). Most plagioclase phenocrysts are zoned normally in terms of Ca, but a few reversally zoned plagioclase phenocrysts cooccur in the same specimens. Phenocryst core compositions for clinopyroxenes and orthopyroxenes in four samples (L 141, M 202, M 354, L 361) show narrow Mg-value ranges with unimodal distributions (Fig. 4). Most of both clino- and ortho-pyroxenes are normally zoned.

3. hornblende-bearing pyroxene andesite

Most of this type occurs as the lavas of the middle unit. They are porphyritic with 36.4–52.7 vol% phenocrysts of plagioclase (29.1–33.3%), clinopyroxene (3.1–4.7%), orthopyroxene (1.1–7.7%), hornblende (0.1–0.2%) and Fe-Ti oxides (1.4–8.5%). These minerals usually show euhedral to subhedral form and occur as

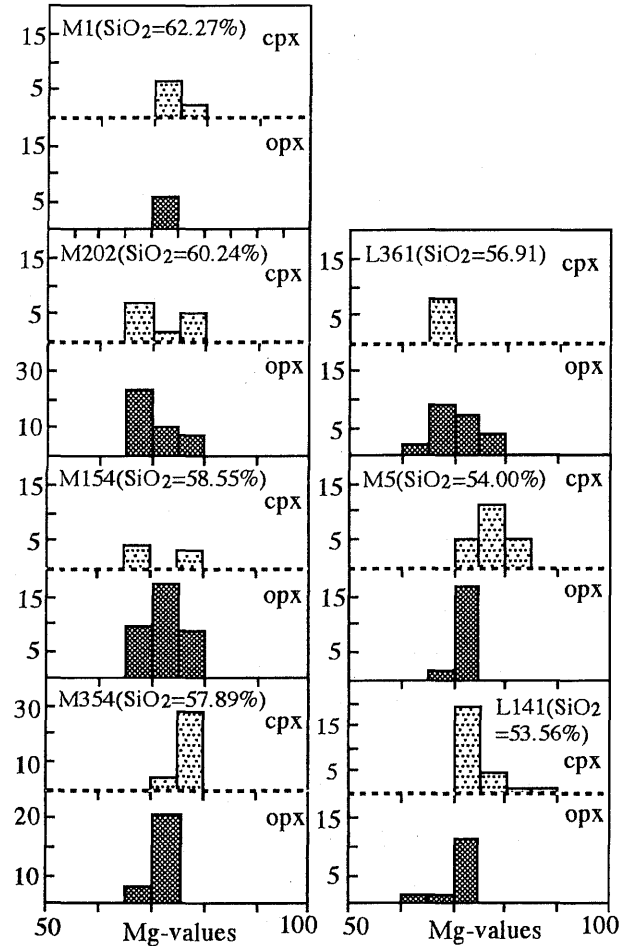


Fig. 4. Frequency of Mg values (Mg/(Mg+Fe)) in the cores of clino- and ortho-pyroxene phenocrysts in the andesites from the Myojin-iwa Formation. SiO₂ contents are those of whole rocks. cpx : clinopyroxene, opx : orthopyroxene.

isolated grains and glomeroporphyritic aggregates of 2–3 mm in diameter.

Plagioclase phenocrysts, 0.5–2.5 mm long, are generally fresh, and a few grains have dusky zones. Clinopyroxene (0.5–1.5 mm long) and orthopyroxene (0.5–1 mm long) phenocrysts are also fresh, but some orthopyroxenes are altered to calcite and clay minerals. Hornblende phenocrysts (less than 0.7 mm in length) have opacite rims. Fe-Ti oxide phenocrysts (less than 0.5 mm across) are mostly titanomagnetite. The groundmass is hyalopilitic or hyalo-ophitic, and consists mainly of plagioclase microlites, Fe-Ti oxides and glass.

Although sample M 63 has plagioclase phenocryst cores with a relatively wide compositional range of An % between 47 and 89, sample M 154 contains plagioclase phenocrysts whose cores show a narrow compositional range from An=42 to An=57 (Fig. 3). These plagioclase phenocrysts are usually normally zoned. The cores of clinopyroxene phenocrysts from sample M 154 show a narrow Mg-value range from 68

to 77, and core compositions for orthopyroxene phenocryst in the same sample also fall within a narrow range of Mg-value between 66 and 78 (Fig. 4). Most clino- and ortho-pyroxenes display weak normal zoning.

4. pyroxene-hornblende andesite

This type is found in the lavas of the middle unit. It is porphyritic with 28.6–36.2 vol% phenocrysts of plagioclase (20.9–30.3%), clinopyroxene (<1.7%), orthopyroxene (0.5–0.8%), hornblende (2.7–4.2%) and Fe-Ti oxides (1.3–2.4%). These minerals usually show euhedral to subhedral shape. They occur mostly as isolated grains, and rarely as glomeroporphyritic aggregates of 2–2.5 mm in diameter.

Plagioclase phenocrysts (0.3–2.5 mm long) are generally fresh, and a few phenocrysts have dusky zones. Clinopyroxene (up to 3mm in length) and orthopyroxene (0.3–1 mm long) phenocrysts are also fresh. Hornblende phenocrysts (0.3–2 mm long) are generally fresh, but most of them have thin opacite rims. They show strong pleochroism of X=pale brown and Y=Z=brown. Fe-Ti oxide phenocrysts (less than 0.5 mm across) are mostly titanomagnetite. The groundmass is hyalopilitic or hyalo-ophitic, containing plagioclase microlites, Fe-Ti oxides and glass.

Sample M1 has phenocryst cores with narrow compositional ranges of An % of 54–63 for plagioclase (Fig. 3), Mg-value of 73–78 for clinopyroxene and Mg-values of 70–72 for orthopyroxene (Fig. 4).

Geochemistry and Sr- and Nd-isotope compositions

1. Major and trace element compositions

Whole rock major- and trace-element analyses were performed for fourteen samples from the lower unit, and twenty-six samples from the middle unit by X-ray fluorescence spectrometry at Niigata University using the analytical methods described by Tamura et al. (1989) and Kawano et al. (1992). The results are listed in Table 2. In the following discussion, the major-element compositions are treated on an anhydrous basis.

The SiO₂ contents of andesitic rocks from the Myojin-iwa Formation vary continuously from 53.3% to 62.8% (Fig. 5). Most of the rocks lie within the high-K andesite field of Gill (1981) (Fig. 5-A), and are comparable to andesitic rocks from the Quaternary Chokai, Oshima-oshima and Kampu volcanoes on the back-arc side (Chokai zone of Nakagawa et al., 1988) of the NE Japan in terms of K₂O content (Hayashi, 1984; Maruyama et al., 1988; Yamamoto, 1988). The compositions of the andesites from the Myojin-iwa Formation are plotted in the high-alkali tholeiite field by Kuno (1968) (Fig. 5-B). In the FeO*/MgO vs. SiO₂ diagram (Fig. 6), they straddle the boundary defining calc-alkaline and tholeiitic fields. The andesitic rocks from the Myojin-iwa Formation are, therefore, regarded in this paper as transitional andesites

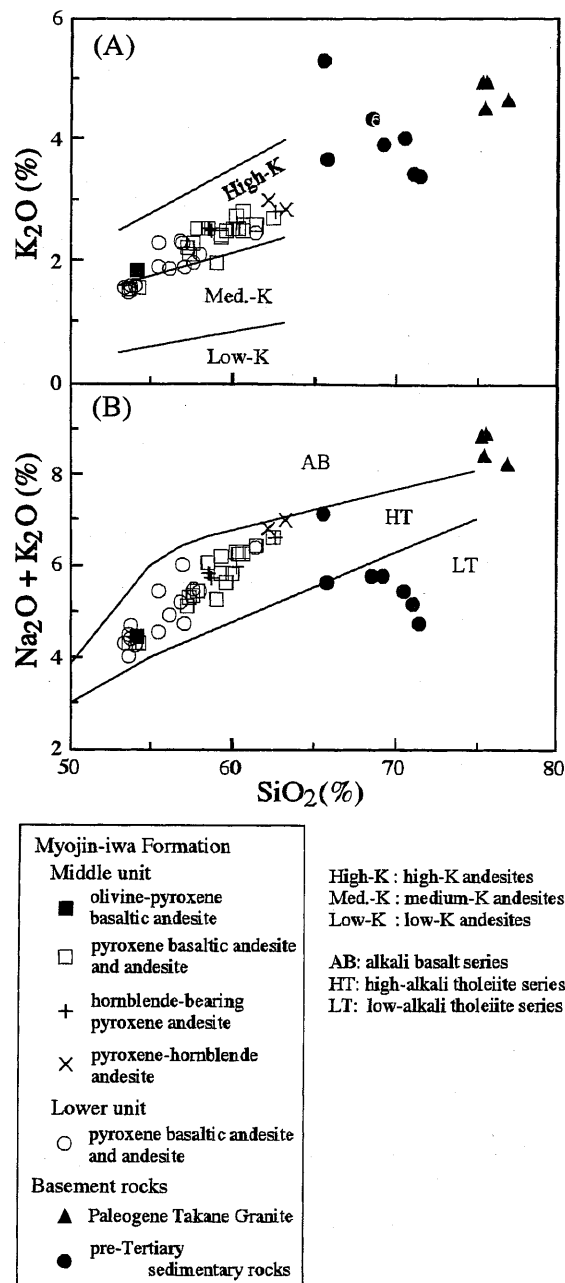


Fig. 5. SiO₂ vs. K₂O and Na₂O+K₂O variation diagrams for the Myojin-iwa Formation and the basement rocks. The fields of low-, med.- and high-K andesites in SiO₂-K₂O diagram are from Gill (1981); the fields of LT (low-alkali tholeiite), HT (high-alkali tholeiite) and AB (alkali basalt) in SiO₂-(Na₂O+K₂O) diagram are from Kuno (1968). Data of the basement rocks in Figs. 5, 6, 8, 9, 11, 12, 13, and 14 are from Rezanov et al. (1999).

between typical calc-alkaline and tholeiitic series. The transitional andesites correspond approximately to rocks of the subordinate tholeiitic series which was distinguished by Kawano et al. (1961) from typical tholeiitic series.

The incompatible element data for the most primitive sample (L139) with an FeO*/MgO ratio of 1.4 are

Table 2. Whole rock chemical compositions of volcanic rocks from the study area.

Sample No.	L193	L182	L180	L141	L139	L138	L134	L106	L293	L123	L294	L361	L136	L105	M6	M5	M150	M101	M116	M92
SiO ₂ (wt%)	52.14	52.77	52.78	52.94	53.72	54.35	54.57	54.96	55.80	56.14	56.45	56.53	56.95	60.71	53.01	53.02	53.05	53.68	53.77	55.47
TiO ₂	1.31	1.46	1.46	1.05	1.00	0.98	1.10	1.23	1.16	1.10	1.13	1.29	1.26	0.80	1.43	1.10	1.11	1.20	1.00	0.92
Al ₂ O ₃	17.47	17.86	17.61	17.62	16.97	17.25	17.92	17.37	17.32	17.48	17.27	17.58	17.83	17.46	17.20	16.44	18.49	18.24	16.70	17.03
FeO*	8.97	8.87	9.05	7.47	7.77	6.32	7.97	7.13	7.51	7.06	7.01	8.08	6.94	5.42	9.53	8.22	8.28	7.94	6.04	6.55
MnO	0.17	0.17	0.18	0.10	0.13	0.13	0.13	0.15	0.16	0.17	0.16	0.16	0.16	0.15	0.19	0.21	0.13	0.16	0.11	0.15
MgO	4.16	3.53	3.96	5.47	5.72	4.99	3.60	4.03	3.54	3.72	3.25	2.53	2.50	2.05	4.09	5.43	4.22	4.18	3.79	3.32
CaO	9.00	8.75	8.77	9.99	9.60	9.29	7.49	7.99	7.41	7.89	7.17	6.89	6.90	5.76	8.63	8.83	9.10	8.94	7.26	7.39
Na ₂ O	2.70	3.04	2.93	2.52	2.64	2.60	3.07	3.00	2.81	2.79	3.45	3.68	3.26	3.87	2.86	2.55	2.75	2.71	2.97	2.94
K ₂ O	1.52	1.59	1.51	1.50	1.61	1.90	2.29	1.84	2.32	1.89	1.97	2.31	2.11	2.48	1.53	1.83	1.52	1.57	2.02	2.23
P ₂ O ₅	0.23	0.24	0.26	0.19	0.19	0.19	0.24	0.23	0.23	0.23	0.24	0.28	0.31	0.22	0.25	0.23	0.21	0.25	0.21	0.23
H ₂ O(±)	1.43	0.94	0.84	0.16	0.30	1.16	0.95	1.20	1.01	1.09	0.94	0.07	0.90	1.25	1.11	1.52	0.77	0.61	5.78	2.69
Total	99.10	99.22	99.35	99.01	99.65	99.16	99.33	99.13	99.27	99.56	99.04	99.40	99.12	100.17	99.83	99.38	99.63	99.48	99.65	98.92
Cr (ppm)	31	7	9	88	90	92	32	18	18	22	12	5	15	34	10	107	18	27	46	30
Nb	7.5	4.4	5.9	6.1	7.8	7.1	9.7	10.6	9.3	9	9	8.9	10.3	11.1	5.1	7.1	4.1	8.5	7.6	9.6
Ni	18	5	8	32	31	26	12	10	11	60	6	3	2	5	9	43	14	14	20	16
Rb	37	34	33	32	31	45	61	45	50	56	49	56	50	65	34	48	23	33	50	62
Sr	342	404	393	406	439	383	322	385	355	364	370	379	423	363	384	319	391	375	372	325
V	225	259	262	200	180	190	190	185	186	186	172	187	174	104	253	197	189	206	175	157
Y	33	31	30	25	41	29	41	37	40	32	40	50	35	35	32	30	24	35	31	32
Zr	107	92	106	94	111	107	138	129	130	129	137	140	141	162	104	119	108	118	131	132
Ba	302	275	291	275	320	323	456	305	320	371	341	399	350	447	268	318	402	342	366	411
Sample No.	M56	M157	M354	M4	M217	M191	M2	M154	M202	M7	M33	M32	M112	M91	M63	M356	M34	M1	M216	M95
SiO ₂ (wt%)	56.26	56.64	56.91	57.32	57.35	57.68	57.72	57.79	58.35	58.55	58.61	58.69	59.12	59.46	59.58	60.52	60.95	61.29	61.33	61.78
TiO ₂	1.24	1.18	1.02	0.98	1.18	1.06	1.08	1.03	0.96	0.99	0.96	1.06	1.02	0.92	1.02	0.98	0.92	0.97	0.84	0.85
Al ₂ O ₃	17.38	18.12	16.81	16.84	17.05	17.47	16.91	17.06	16.94	16.79	17.21	16.89	17.81	16.81	17.09	17.22	16.69	17.26	17.23	17.58
FeO*	6.69	7.18	7.47	6.93	7.44	6.91	6.77	6.95	5.56	6.35	6.30	6.27	5.43	6.07	5.88	5.98	5.83	4.87	5.01	4.33
MnO	0.15	0.10	0.15	0.18	0.17	0.17	0.20	0.12	0.14	0.16	0.20	0.16	0.09	0.16	0.12	0.20	0.16	0.15	0.15	0.14
MgO	2.15	3.31	3.26	2.96	3.36	2.17	2.37	2.89	2.45	3.16	1.73	1.64	2.53	2.32	2.64	1.74	1.24	1.54	1.58	0.90
CaO	6.21	7.17	7.07	6.60	5.17	5.96	6.01	6.87	5.97	6.60	5.81	5.67	6.70	5.84	6.29	5.26	4.71	5.31	5.17	5.00
Na ₂ O	3.35	2.89	2.88	3.16	3.20	3.32	3.66	3.23	3.46	3.08	3.59	3.61	3.20	3.40	3.30	3.78	3.70	3.73	3.84	4.05
K ₂ O	2.48	2.21	2.51	2.47	1.95	2.38	2.40	2.53	2.67	2.50	2.48	2.46	2.55	2.78	2.63	2.58	2.78	2.98	2.70	2.80
P ₂ O ₅	0.35	0.26	0.23	0.23	0.30	0.24	0.27	0.23	0.36	0.23	0.24	0.28	0.23	0.22	0.24	0.26	0.26	0.32	0.28	0.30
H ₂ O(±)	3.09	1.81	1.00	1.43	1.92	2.24	1.91	0.60	2.33	0.85	1.97	2.51	0.50	1.17	0.67	0.82	1.90	1.37	1.53	1.49
Total	99.35	100.87	99.31	99.10	99.09	99.60	99.30	99.30	99.19	99.26	99.10	99.24	99.18	99.15	99.46	99.34	99.14	99.79	99.66	99.22
Cr (ppm)	2	17	18	25	3	9	7	19	6	23	17	1	23	18	20	2	1	6	1	2
Nb	11.9	6.7	7.3	9.7	8.7	9.3	12	10.2	11.3	9.6	11.3	11.1	9.9	9.8	10.6	8.6	12.8	11.8	8.8	11.9
Ni	3	18	9	11	5	4	35	9	4	8	14	37	11	8	12	3	3	9	3	2
Rb	62	66	66	67	34	57	59	69	72	68	60	61	73	79	74	66	72	70	67	72
Sr	413	358	340	311	342	355	346	355	318	330	341	356	336	298	313	357	328	385	356	378
V	191	181	166	161	158	168	162	172	158	166	141	164	158	134	150	129	128	131	113	112
Y	43	34	41	36	35	35	32	40	32	40	43	40	43	39	40	34	48	46	38	43
Zr	152	142	130	145	144	144	155	136	162	154	159	156	152	164	159	152	176	174	178	182
Ba	399	475	411	422	414	416	390	479	456	454	465	497	469	453	455	483	503	438	487	495

L193-L105; rocks of the lower unit, M6-M95; rocks of the middle unit. L193-L105; pyroxene basaltic andesite and andesite, M4, M154, M63, M34; hornblende-bearing pyroxene andesite, M6, M150-M354, M217-M2, M202-M91, M356, M216; pyroxene basaltic andesite and andesite, M5; olivine-pyroxene basaltic andesite, M1, M95; pyroxene-hornblende andesite. FeO* = FeO+0.9Fe₂O₃.

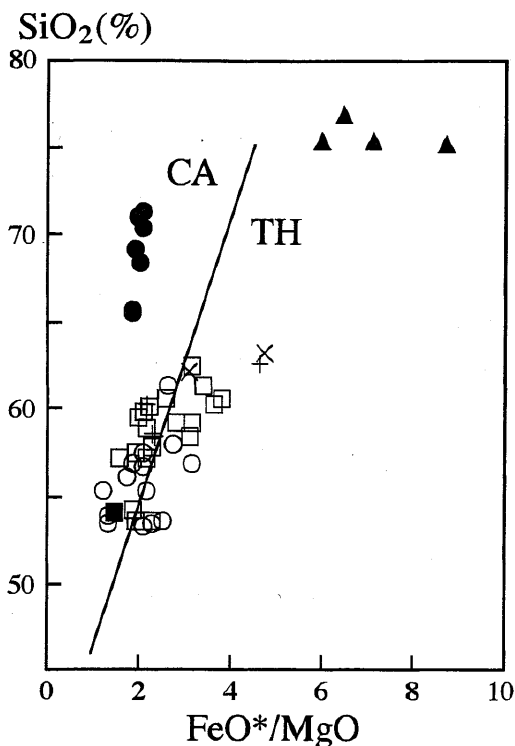


Fig. 6. FeO*/MgO vs. SiO₂ diagram for the Myojin-iwa Formation and the basement rocks. Line shows the boundary between the fields of calc-alkaline series (CA) and tholeiitic series (TH) (after Miyashiro, 1974). Symbols are the same as Fig. 5.

plotted on a conventional N-MORB normalized spidergram (Fig. 7) together with data for the Pliocene and Quaternary basaltic rocks from the back-arc side of the NE Japan. One of the most conspicuous geochemical characteristics of island-arc basalts is their positive anomalies of LIL elements such as Ba, Rb and K, and their negative anomalies of HFS elements such as Nb and Zr, as shown on the primordial mantle or N-MORB normalized patterns for incompatible elements (e.g., Sun and Nesbitt, 1977 ; Pearce, 1983).

Fig. 7 shows that both the Pliocene and Quaternary basaltic rocks (including the basaltic andesites) from the back-arc side of NE Japan have similar incompatible element patterns, with positive Ba, K and Rb anomalies and a negative Nb anomaly. Supposing considerable degree of partial melting, these chemical features suggest that chemical characteristics of the source materials was similar for both the Pliocene and Quaternary basaltic rocks in the back-arc side of the NE Japan.

As shown in Figs. 5 and 8, TiO₂, FeO*, MgO, CaO, Na₂O, P₂O₅ and K₂O contents of andesites from the Myojin-iwa area plot near the linear trends on the SiO₂ variation diagrams. In contrast, the SiO₂-Al₂O₃ and MnO diagrams show nearly constant Al₂O₃ and MnO contents despite of increase in SiO₂ content (Fig. 8).

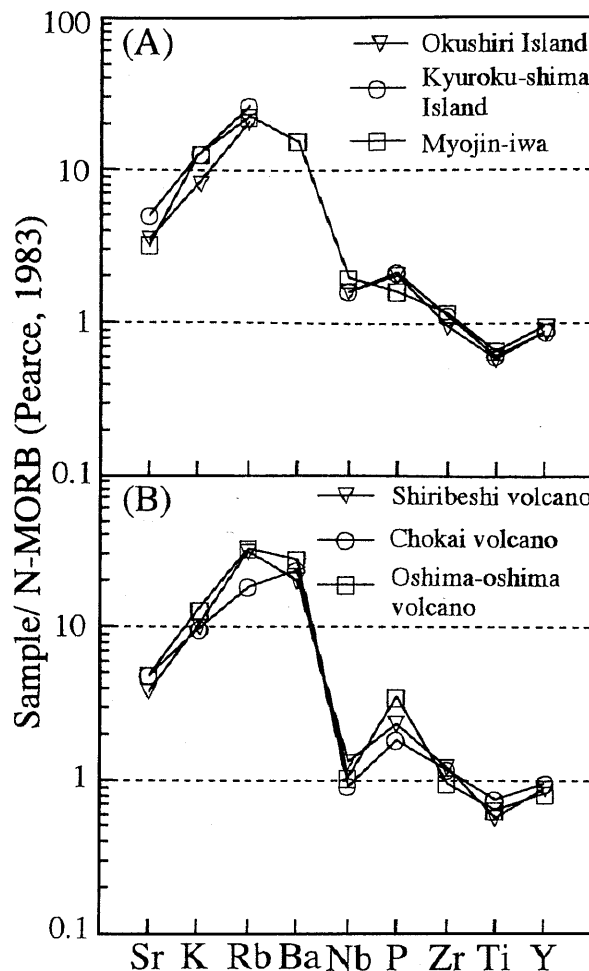


Fig. 7. Abundance patterns of incompatible elements in the Pliocene basalts and basaltic andesites (A) and the Quaternary basalts (B), normalized to N-type MORB of Pearce (1983). Data sources : Okushiri Island (Yamamoto et al., 1991), Kyuroku-shima Island (Fukudome et al., 1990), Shiribeshi volcano (Tsuchiya and Shuto, 1993), Chokai volcano (Hayashi, 1986), Oshima-oshima volcano (Yoshida and Aoki, 1988), Myojin-iwa (this study).

Linear variation trends are also recognized in the SiO₂ versus trace element variation diagrams (Fig. 9). Ba, Rb, Nb, Y, Zr and V contents of andesites from the Myojin-iwa Formation gradually increase or decrease with the increase in SiO₂, whereas Sr contents of the andesites do not show large variation with increasing SiO₂ content.

2. Sr and Nd isotope compositions

A. Analytical procedures

The extraction of Rb, Sr, Sm and Nd from rock powder has been described by Kagami et al. (1987). Mass spectrometric analyses follow the procedures of Kagami et al. (1987, 1989) and Miyazaki and Shuto (1998). Mass spectrometric analyses were conducted using a MAT262 mass spectrometer at Niigata University. ⁸⁷Sr/⁸⁶Sr and ¹⁴³Nd/¹⁴⁴Nd ratios were normalized to ⁸⁶Sr/⁸⁸Sr=0.1194 and ¹⁴⁶Nd/¹⁴⁴Nd=

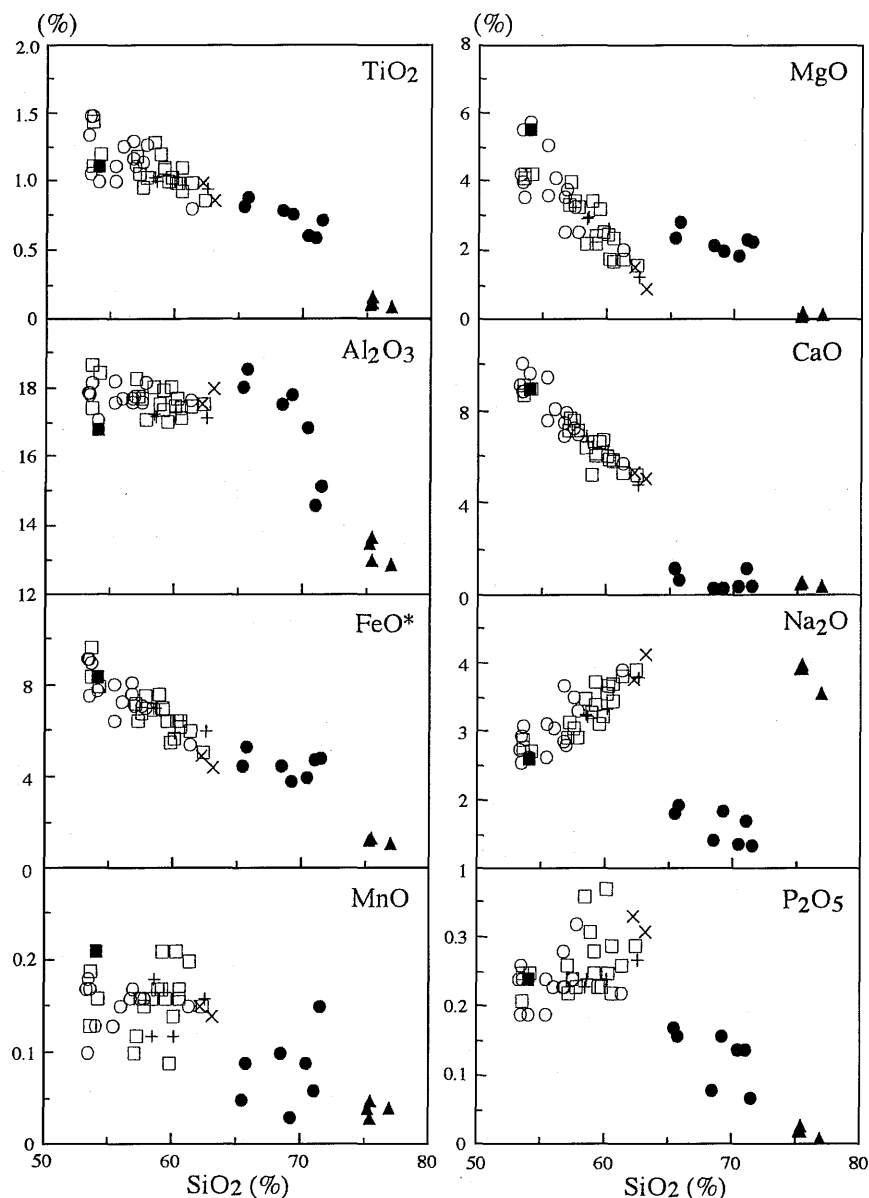


Fig. 8. SiO_2 vs. major element variation diagram. Symbols are the same as Fig. 5.

0.7219, respectively. Blanks tested throughout the present analytical procedure yielded 1.0 ng for Sr, 0.06 ng for Sm and 0.6 ng for Nd.

Sr isotope ratios for NBS 987 were measured ten times during this study, producing an average ratio of 0.710251 ± 0.000003 (2σ , $N=51$). Rb and Sr concentrations were determined by X-ray fluorescence. The mean $^{143}\text{Nd}/^{144}\text{Nd}$ ratio of JB-1 a during this study was 0.512782 ± 0.000007 (2σ , $N=9$). During the course of this study, we also measured $^{143}\text{Nd}/^{144}\text{Nd}$ ratios of two the La Jolla and JNdi-1 standards, the latter of which is a new standard provided by the Geological Survey of Japan. The La Jolla standard gave a mean $^{143}\text{Nd}/^{144}\text{Nd}$ ratio of 0.511851 ± 0.000006 (2σ , $N=17$) and JNdi-1 standard a mean $^{143}\text{Nd}/^{144}\text{Nd}$ ratio of 0.512106 ± 0.000003 (2σ , $N=44$). The authors used the following CHUR parameters for calculation of initial ϵ_{Sr} and ϵ_{Nd}

values: $^{87}\text{Sr}/^{86}\text{Sr}(\text{present})=0.7045$, $^{87}\text{Rb}/^{86}\text{Sr}(\text{present})=0.0827$, $\lambda^{87}\text{Rb}=1.42 \times 10^{-11} \text{y}^{-1}$, $^{143}\text{Nd}/^{144}\text{Nd}(\text{present})=0.512638$, $^{147}\text{Sm}/^{144}\text{Nd}(\text{present})=0.1966$, $\lambda^{147}\text{Sm}=6.54 \times 10^{-12} \text{y}^{-1}$.

B. Results

The analytical results and initial Sr and Nd isotope ratios, calculated assuming the formation age to be 3 Ma, are presented in Table 3. In this paper, initial Sr and Nd isotope ratios are hereafter referred to SrI and NdI , respectively.

Thirty-eight specimens from the Myojin-iwa Formation have SrI values between 0.70323 and 0.70378, and twenty-three specimens have NdI values between 0.512791 and 0.512926 (Table 3). The SrI values display positive correlations with SiO_2 (Fig. 10-A), whereas NdI values gradually decrease with increasing SiO_2 (Fig. 10-B). These Sr and Nd isotope data are plotted

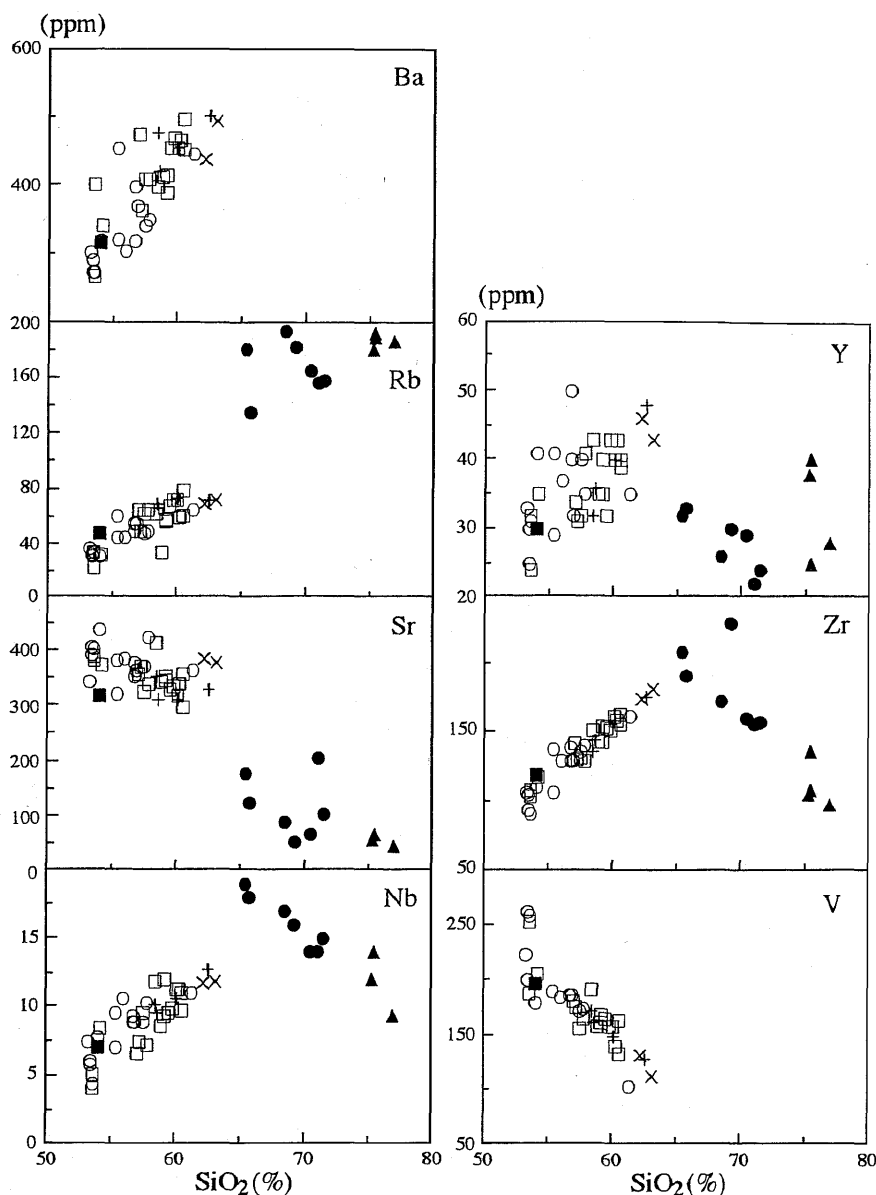


Fig. 9. SiO₂ vs. trace element variation diagram. Symbols are the same as Fig. 5.

in terms of initial $\epsilon\text{Sr}-\epsilon\text{Nd}$ (Fig. 11), and seem to vary along the schematic Mantle Array of DePaolo (1988).

The lowest SrI (~ 0.7032) value recorded is slightly higher than Sr I values previously reported from the Pliocene to Quaternary basaltic rocks from the back-arc side of the NE Japan (Chokai volcano; 0.70291, Kampu volcano; ~ 0.7030 , Oshima-oshima volcano; ~ 0.7031 ; Shiribeshi volcano; ~ 0.7030 ; Okushiri Island; ~ 0.7030) (Shuto et al., 1991, 1993; Ohki et al., 1994). This suggests that these back-arc side basaltic magmas were derived from mantle sources with small heterogeneity in Sr isotope composition.

Discussion

Major and trace element contents of the andesites from the Myojin-iwa area mostly plot as almost straight lines or curves in conventional SiO₂-variation

diagrams (Figs. 5, 8 and 9). These compositional trends could result from fractional crystallization, magma mixing or crustal assimilation combined with fractional crystallization. The phenocrystic minerals in most rocks from the Myojin-iwa Formation are characterized by 1) unimodal core compositions for most clinopyroxene, orthopyroxene and plagioclase phenocrysts, 2) mostly normal zoning of these phenocrysts, and 3) no disequilibrium phenocryst assemblages such as olivine and quartz. These facts suggest that the andesites have not been largely affected by magma mixing.

The variations of Nb versus Zr for the basaltic andesite and andesite from the Myojin-iwa area are shown in Fig. 12, together with the data for the pre-Tertiary shales and the granitoid rocks of the Paleogene Takene Granite, situated 15 km east of the

Table 3. Sr and Nd isotopic data for volcanic rocks from the study area.

Sample number	$^{87}\text{Rb}/^{86}\text{Sr}$	$^{87}\text{Sr}/^{86}\text{Sr}$	SrI(3Ma)	Sm (ppm)	Nd (ppm)	$^{147}\text{Sm}/^{144}\text{Nd}$	$^{143}\text{Nd}/^{144}\text{Nd}$	NdI(3Ma)
L193	0.313	0.703430±13	0.703417±13	4.68	18.3	0.1546	0.512914±10	0.512911±10
L182	0.243	0.703473±12	0.703463±12	nd	nd	nd	nd	nd
L180	0.243	0.703500±12	0.703490±12	4.78	18.50	0.1563	0.512914±13	0.512911±13
L141	0.228	0.703248±11	0.703238±11	3.87	15.6	0.1506	0.512929±12	0.512926±12
L139	0.204	0.703301±13	0.703292±13	4.95	18.7	0.1597	0.512906±15	0.512903±15
L138	0.340	0.703376±11	0.703362±11	nd	nd	nd	0.512942±10	nd
L134	0.548	0.703549±15	0.703526±15	nd	nd	nd	nd	nd
L106	0.338	0.703542±12	0.703528±12	nd	nd	nd	0.512919±11	nd
L293	0.407	0.703569±12	0.703552±12	nd	nd	nd	0.512880±12	nd
L123	0.445	0.703524±14	0.703505±14	nd	nd	nd	nd	nd
L294	0.383	0.703562±11	0.703546±11	nd	nd	nd	0.512897±14	nd
L361	0.427	0.703466±12	0.703448±12	nd	nd	nd	0.512897±12	nd
L136	0.342	0.703547±13	0.703532±13	nd	nd	nd	0.512897±11	nd
L105	0.518	0.703459±14	0.703437±14	nd	nd	nd	nd	nd
M6	0.256	0.703502±15	0.703491±15	4.62	17.8	0.1571	0.512919±13	0.512916±13
M5	0.435	0.703520±12	0.703501±12	4.61	19.2	0.1451	0.512848±13	0.512845±13
M150	0.170	0.703338±13	0.703331±13	4.51	18.3	0.1487	0.512934±14	0.512931±14
M101	0.255	0.703422±12	0.703411±12	4.85	19.9	0.1476	0.512901±14	0.512898±14
M116	0.389	0.703423±11	0.703406±11	4.67	11.3	0.2502	0.512926±10	0.512921±10
M92	0.552	0.703595±12	0.703571±12	5.34	22.7	0.1422	0.512817±10	0.512814±10
M56	0.434	0.703634±12	0.703615±12	6.02	25.2	0.1444	0.512898±11	0.512895±11
M157	0.533	0.703505±13	0.703482±13	5.49	22.8	0.1460	0.512903±12	0.512900±12
M354	0.561	0.703335±14	0.703311±14	5.34	23.1	0.1396	0.512921±14	0.512918±14
M4	0.623	0.703699±12	0.703672±12	nd	nd	nd	0.512811±12	nd
M217	0.288	0.703653±11	0.703641±11	nd	nd	nd	nd	nd
M191	0.464	0.703479±15	0.703459±15	5.22	21.9	0.1442	0.512902±11	0.512899±11
M2	0.493	0.703616±13	0.703595±13	5.96	24.8	0.1455	0.512884±15	0.512881±15
M154	0.562	0.703402±12	0.703378±12	nd	nd	nd	nd	nd
M202	0.655	0.703633±12	0.703605±12	5.77	24.6	0.1421	0.512904±17	0.512901±17
M7	0.596	0.703663±14	0.703638±14	nd	nd	nd	nd	nd
M33	0.509	0.703616±11	0.703594±11	5.85	24.5	0.1441	0.512794±12	0.512791±12
M32	0.496	0.703673±10	0.703652±10	6.25	25.9	0.1460	0.512881±11	0.512878±11
M112	0.628	0.703665±13	0.703638±13	6.82	29.7	0.1388	0.512826±13	0.512823±13
M91	0.767	0.703808±12	0.703775±12	5.62	24.3	0.1398	0.512828±12	0.512825±12
M63	0.684	0.703724±11	0.703695±11	5.59	24.1	0.1406	0.512843±10	0.512840±10
M34	0.635	0.703705±13	0.703678±13	nd	nd	nd	nd	nd
M1	0.526	0.703518±12	0.703496±12	6.67	28.9	0.1396	0.512881±14	0.512878±14
M95	0.551	0.703569±13	0.703546±13	5.89	25.2	0.1415	0.512889±12	0.512886±12

SrI ; initial $^{87}\text{Sr}/^{86}\text{Sr}$ ratio, NdI ; initial $^{143}\text{Sr}/^{144}\text{Sr}$ ratio. SrI and NdI values are calculated assuming a formation age of 3Ma (deduced from K-Ar age reported by Agency of Natural Resources and Energy, 1982). Rb and Sr contents are shown in Table 2.

study area by Rezanov et al. (1999). Assuming the phenocrysts (olivine, clinopyroxene, orthopyroxene, plagioclase, hornblende and Fe-Ti oxide) observed in the andesitic samples as the fractionating phases, D_{Nb} (the bulk distribution coefficient for Nb) would be equal to or higher than D_{Zr} (e.g., Pearce and Norry, 1979; Rollinson, 1993). Thus, the Zr/Nb for differentiated magmas should be equal to or higher than that for the less differentiated magmas. Howev-

er, the andesites have lower Zr/Nb ratios (20–10) than the basaltic andesites (30–20) (Fig. 12), suggesting that the origin of the andesites cannot be explained simply by the fractional crystallization of the basaltic andesite magma. Crustal materials, such as the pre-Tertiary sedimentary rocks and Paleogene granitoid rocks with lower Zr/Nb ratios than those of the Myojin-iwa andesitic rocks, might be involved in their origin to decrease the Zr/Nb ratios of the andesitic rocks (Fig. 12).

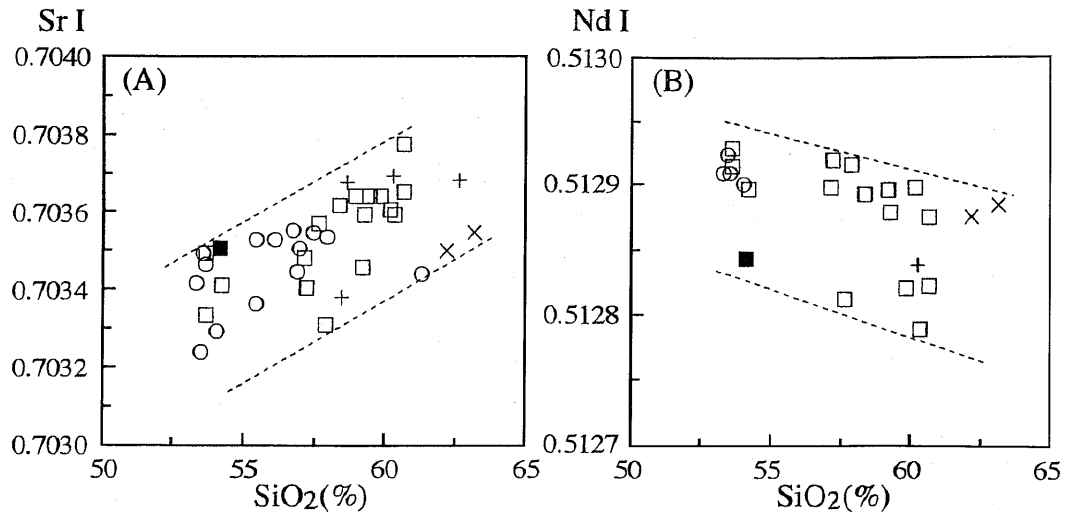


Fig. 10. SiO₂ vs. SrI and SiO₂ vs. NdI diagrams for volcanic rocks from the study area. Symbols are the same as Fig. 5.

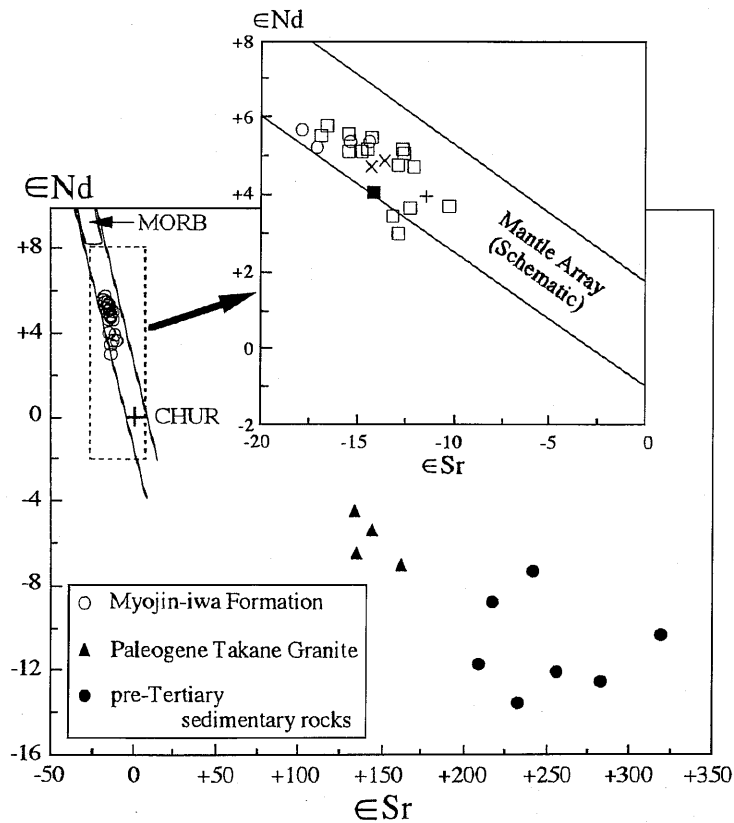


Fig. 11. Initial ϵ Sr and ϵ Nd diagrams. MORB and schematic mantle array are after DePaolo (1988). Symbols are the same as Fig. 5.

The correlations between the SiO₂ contents and SrI- and NdI-values (Fig. 10), and the Sr and Nd isotope variations in Fig. 11 for the Myojin-iwa andesitic rocks cannot be also explained in terms of simple fractional crystallization of basaltic magma, but may provide strong evidences for the operation of an as-

simulation and fractional crystallization (AFC) process (e.g., DePaolo, 1981 ; Roberts and Clemens, 1995). We have examined, therefore, the possible effects of upper-crustal materials on the genesis of the andesites from the Myojin-iwa Formation.

Geological and seismological data suggest that the

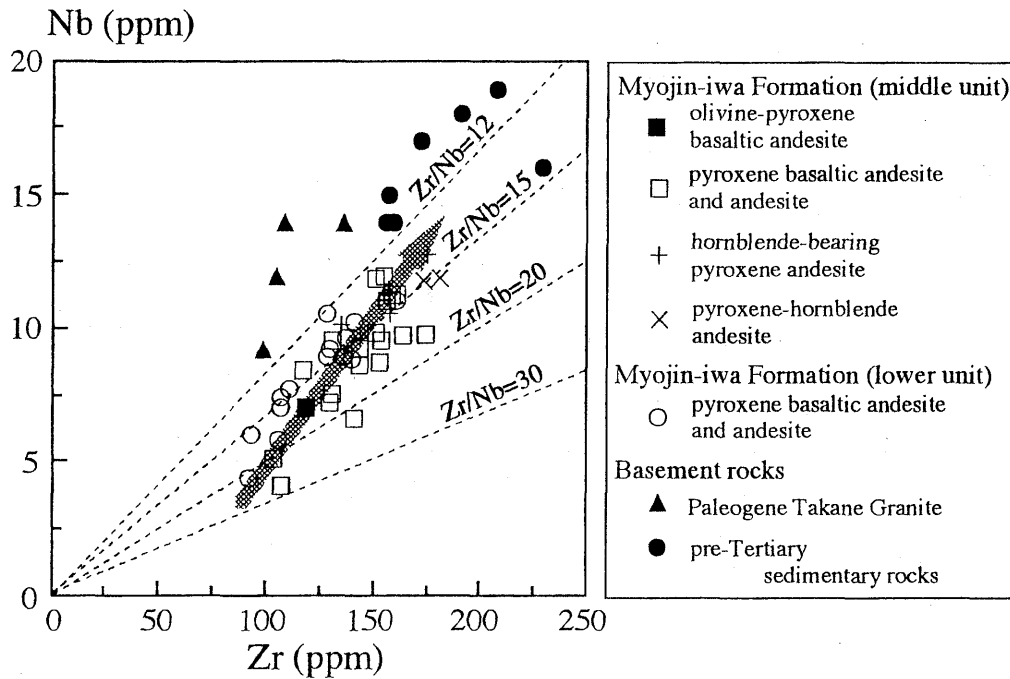


Fig. 12. Nb vs. Zr diagram for volcanic rocks from the study area and the basement rocks. The arrow represents the general trend in the andesites from the study area.

upper part of the crust (i.e. less than 15 km depth) in the Myojin-iwa and surrounding areas is composed mainly of the pre-Tertiary sedimentary rocks and Cretaceous-Paleogene granitoid rocks (Agency of Natural Resources and Energy, 1982; Niigata Prefecture, 1989). The pre-Tertiary sedimentary rocks in the northern part of the Niigata area are composed mainly of shale and sandstone with lesser amounts of basic volcanics, chert and limestone. Mizutani et al. (1984) described Jurassic radiolarians from siliceous shale in the Tsugawa area, Niigata Prefecture, and noted that the pre-Tertiary sedimentary rocks in the Tsugawa and surrounding areas are the correlatives of the middle and late Jurassic formations of the Mino, Ashio and Yamizo areas. Cretaceous-Paleogene granitoid rocks intrude this pre-Tertiary sedimentary rocks.

Zr/Nb ratios and Sr- and Nd-isotope data indicate upper-crustal assimilation as an important petrogenetic process during the generation of the andesites of the Myojin-iwa area. In order, therefore, to evaluate the role of AFC in the generation of the andesites, we examined the effects of AFC on the Nd isotope ratios and associated Nb and Nd abundances using the equations of DePaolo (1981).

In this calculation, the initial basaltic magma was assumed to have had Nd isotope ratio (at 3 Ma) = 0.512950, Nd = 10 ppm and Nb = 4 ppm. These Nd isotope ratio, and Nd and Nb abundances correspond to those which are slightly higher than the highest Nd isotope ratio at 3 Ma (0.512926) of the andesites from the Myojin-iwa Formation and are slightly lower than the lowest abundances of Nd (11.3 ppm) and Nb (4.1

ppm), respectively (Tables 2 and 3). The assimilants were assumed to have had Nd isotope ratio (at 3 Ma) = 0.512081, Nd = 30 ppm and Nb = 16 ppm for the pre-Tertiary sedimentary rocks (average values of seven shales in Table 2 of Rezanov et al. (1999)), and Nd isotope ratio (at 3 Ma) = 0.512340, Nd = 29 ppm and Nb = 12 ppm for the Paleogene Takane Granite (average values of four granitoid rocks in Table 1 of Rezanov et al. (1999)). The bulk distribution coefficient for the fractionating assemblage (olivine; 1 vol%, clinopyroxene; 20%, orthopyroxene; 9%, Fe-Ti oxide; 2% and plagioclase; 68%-average phenocryst modal value of five basaltic andesite samples, L 141, L 138, M 5, M 6 and M 150 in Table 1) was assumed to have been 0.03 for Nb and 0.16 for Nd. The distribution coefficient values for these elements were taken from Table 4.1 of Rollinson (1993).

The results of the AFC calculations are shown in Fig. 13, in which simple mixing curves are also illustrated for comparison with the AFC results. Fig. 13 shows that the Nb, Nd and NdI variations in the andesites from the Myojin-iwa Formation can be explained by AFC trajectories, but not by simple mixing pathways. It seems from Fig. 14 that both the pre-Tertiary sedimentary rocks and the Paleogene granitoid rocks were probable assimilants.

In general, andesitic rocks of the calc-alkaline series tend to have abundant phenocrysts of Fe-Ti oxide than those of the tholeiitic series (e.g., Ewart, 1982). For example, tholeiitic andesites from a Quaternary Adataro volcano, NE Japan contain 0.3–1.5 vol% of Fe-Ti oxide phenocrysts, whereas calc-alkaline andesites from the same volcano contain 0.6–2.6 vol% of

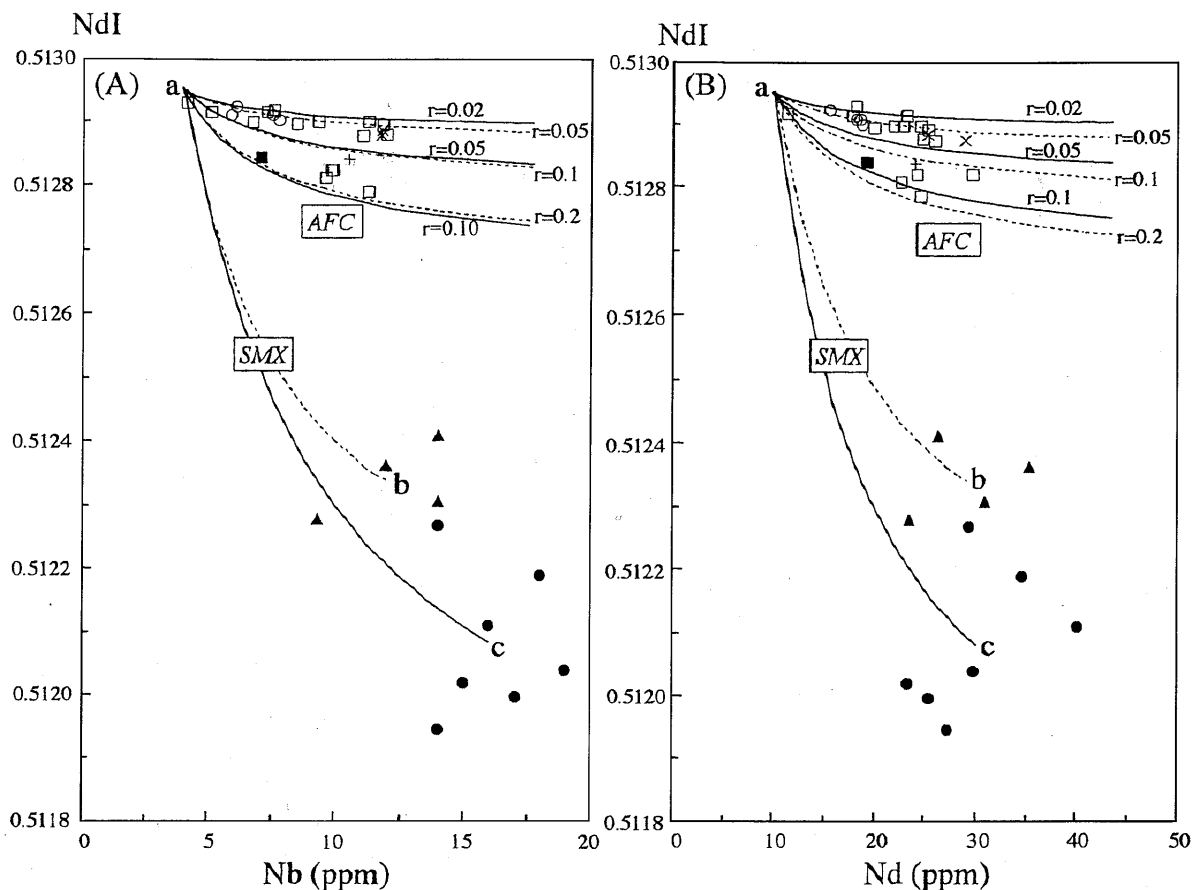


Fig. 13. NdI vs. Nb and NdI vs. Nd diagrams. SMX=calculated simple mixing trajectories between basaltic magma and pre-Tertiary sedimentary rocks (solid line), and basaltic magma and the Paleogene Takane Granite (broken line); AFC=trajectories of fractional crystallization with assimilation of the pre-Tertiary sedimentary rocks (solid line) and the Paleogene Takane Granite (broken line); r =ratio of assimilation to crystallization rates. Parameters used in this calculation are described in the text. Symbols are the same as Fig. 12. End member parameters; basaltic magma (a): NdI=0.51290, Nd=10 ppm, Nb=4 ppm, Paleogene Takane Granite (b): NdI=0.512340, Nd=29 ppm, Nb=12 ppm, pre-Tertiary sedimentary rocks (average values of seven samples) (c): NdI=0.512081, Nd=30 ppm, Nb=16 ppm.

these phenocrysts (Fujinawa, 1990). The modal abundances of Fe-Ti oxide phenocrysts in the andesites from the Myojin-iwa area are 0.8–8.5% (Table 1). Such high values are the characteristics of the calc-alkaline andesites.

However, the geochemical data of the Myojin-iwa andesites are not necessarily typical to those of the calc-alkaline rocks (Fig. 6). They plot on the variation line which obliquely intersects the boundary between the calc-alkaline and tholeiitic fields. This suggests that the FeO^*/MgO ratios of the andesites from the Myojin-iwa Formation were affected by assimilation of the Paleogene granitoid rocks with higher FeO^*/MgO ratios rather than the pre-Tertiary sedimentary rocks with lower FeO^*/MgO ratios (Fig. 6). Consequently, we can choose the Paleogene granitoid rocks as assimilants for the AFC in the generation of the andesites from the Myojin-iwa Formation. However, a basaltic andesite M5 with low FeO^*/MgO ratio is plotted near AFC line with $r=0.2$ (Fig. 13). This is not

clear but may be explained by heterogeneity in Nd isotope ratios of the primary basaltic magma.

The data ranges of the Myojin-iwa andesites can be explained by values of r (ratio of the rate of assimilation to the rate of fractional crystallization) less than 0.2.

Acknowledgements

The authors express their sincere thanks to Messrs. T. Takahashi and T. Miyazaki of Niigata Univ. for their help with the analysis of major and trace elements, and Sr and Nd isotopes. We are also indebted to Dr. R.W. Gallois of the British Geological Survey for his revision of the English.

References

Agency of Natural Resources and Energy, 1982, *Report of regional geological survey of Uetsu district (I)*, 164 p.**
 Anderson, A.T., 1976, Magma mixing: petrological process and volcanological tool. *Jour. Volcanol. Geotherm. Res.*, 1,

- 3–33.
- DePaolo, D.J., 1981, Trace element and isotopic effects of combined wallrock assimilation and fractional crystallization. *Earth Planet. Sci. Lett.*, **53**, 189–202.
- DePaolo, D.J., 1988, *Neodymium isotope geochemistry*. Springer-Verlag, 187 p.
- Eichelberger, J.C., 1975, Origin of andesite and dacite: evidence of mixing at Glass Mountain in California and the other circum-Pacific volcanoes. *Bull. Geol. Soc. Amer.*, **86**, 1381–1391.
- Ewart, A., 1982, The mineralogy and petrology of Tertiary-Recent orogenic volcanic rocks: with special reference to the andesite-basaltic compositional range. In Thorpe, R.S., ed., *Andesites: Orogenic andesites and related rocks*, John Wiley & Sons, 25–87.
- Fujimaki, K. and Kurasawa, H., 1980, Lateral variation of REE patterns of basaltic magma across the Japan arc. *Jour. Japan. Assoc. Mineral. Petrol. Econ. Geol.*, **75**, 313–322.
- Fujinawa, A., 1990, Tholeiitic and calc-alkaline magma series at Adataro volcano, northeast Japan: 1. Geochemical constraints on their origin. *Lithos*, **22**, 135–158.
- Fukudome, T., Yoshida, T., Nagao, K., Itaya, T. and Tanoue, S., 1990, Pliocene alkali basalt from Kyuroku-shima Island, northeast of Japan Sea. *Jour. Mineral. Petrol. Econ. Geol.*, **85**, 10–18.*
- Gill, J., 1981, *Orogenic andesite and plate tectonics*. Springer-Verlag, 390 p.
- Hayashi, S., 1984, Petrology of Chokai volcano. Part I—Petrography and major element compositions—. *Jour. Japan. Assoc. Mineral. Petrol. Econ. Geol.*, **79**, 475–483.*
- Hayashi, S., 1986, Petrology of Chokai volcano. Part III—Trace elements and petrogenesis—. *Jour. Japan. Assoc. Mineral. Petrol. Econ. Geol.*, **81**, 370–383.*
- James, D.E., 1982, A combined O, Sr, Nd and Pb isotopic and trace element study of crustal contamination. *Earth Planet. Sci. Lett.*, **57**, 47–62.
- Kagami, H., Iwata, M., Sano, S. and Honma, H., 1987, Sr and Nd isotopic compositions and Rb, Sr, Sm, and Nd concentrations of standard samples. *Tech. Rep. ISEI. Okayama Univ.*, Ser. B, no. 4, 16 p.
- Kagami, H., Yokose, H. and Honma, H., 1989, $^{87}\text{Sr}/^{86}\text{Sr}$ and $^{143}\text{Nd}/^{144}\text{Nd}$ ratios of GSJ rock reference samples; JB-1 a, JA-1 and JG-1 a. *Geochem. Jour.*, **23**, 209–214.
- Kawano, Y., Watanabe, N., Yamamoto, K. and Shuto, K., 1992, Quantitative analysis of Ba, Co, Cr and V in silicate rocks by X-ray fluorescence method. *Contrib. Dept. Geol. Min. Niigata Univ.*, no. 7, 111–115.*
- Kawano, Y., Yagi, K. and Aoki, K., 1961, Petrography and petrochemistry of the volcanic rocks of Quaternary volcanoes of northeastern Japan. *Sci. Rep. Tohoku Univ.*, Ser. III, **7**, 1–46.
- Koyaguchi, T. Blake, S., 1989, The dynamics of magma mixing in a rising magma batch. *Bull. Volcanol.*, **52**, 127–137.
- Kuno, H., 1960, High-alumina basalt. *Jour. Petrol.*, **1**, 121–145.
- Kuno, H., 1968, Discussion of paper by H. Aoki and M. Ito, "Rocks in the oceanic region—I. High-alumina basalts—" *Earth Science (Chikyu Kagaku)*, **22**, 195–197.**
- Maruyama, T., Yamamoto, M. and Yoshioka, S., 1988, Geology and Petrology of Kampo volcano, Oga Peninsula, Japan. *Rep. Res. Inst. Natural Resources, Min. Coll. Akita Univ.*, no. 55, 23–34.*
- Masuda, Y., 1979, Lateral variation of trace element content in Quaternary volcanic rocks across Northeast Japan. *Bull. Univ. Osaka Pref.*, Ser. A, **28**, 105–124.
- Miyashiro, A., 1974, Volcanic rock series in island arcs and active continental margins. *Amer. Jour. Sci.*, **275**, 265–277.
- Miyazaki, T. and Shuto, K., 1998, Sr and Nd isotope ratios of twelve GSJ rock reference samples. *Geochem. Jour.*, **32**, 345–350.
- Mizutani, S., Uemura, T. and Yamamoto, H., 1984, Jurassic radiolarians from the Tsugawa area, Niigata Prefecture, Japan. *Earth Science (Chikyu Kagaku)*, **38**, 352–358.
- Nakagawa, M., Shimotori, H., Yoshida, T., 1986, Aoso-Osore volcanic zone—the front of Northeast Honshu arc, Japan. *Jour. Japan. Assoc. Mineral. Petrol. Econ. Geol.*, **81**, 471–478.*
- Nakagawa, M., Shimotori, H., Yoshida, T., 1988, Across-arc compositional variation of the Quaternary basaltic rocks from the Northeast Japan arc. *Jour. Japan. Assoc. Mineral. Petrol. Econ. Geol.*, **83**, 9–25.*
- Nakajima, S., Shuto, K., Kagami, H., Ohki, J. and Itaya, T., 1995, Across-arc chemical and isotopic variation of Late Miocene to Pliocene volcanic rocks from the Northeast Japan arc. *Mem. Geol. Soc. Japan*, no. 44, 197–226.*
- Niigata Prefecture, 1989, Geological Map of Niigata Prefecture at 1:200000. 177 p.
- Ohki, J., Shuto, K. and Kagami, H., 1994, Middle Miocene bimodal volcanism by asthenospheric upwelling: Sr and Nd isotopic evidence from the back-arc region of the Northeast Japan arc. *Geochem. Jour.*, **28**, 473–487.
- Pearce, J.A., 1983, Role of the sub-continental lithosphere in magma genesis at active continental margins. In Hawkesworth, C.J. and Norry, M.J., eds., *Continental basalts and mantle xenoliths*, Shiva, Nantwich, 230–249.
- Pearce, J.A. and Norry, M.J., 1979, Petrogenetic implications of Ti, Zr, Y, and Nb variations in volcanic rocks. *Contrib. Mineral. Petrol.*, **69**, 33–47.
- Petrini, R., Civetta, L., Piccirillo, E.M., Bellieni, G., Comin-Chiaromonte, P., Marques, L.S. and Melfi, A.J., 1987, Mantle heterogeneity and crustal contamination in the genesis of low-Ti continental flood basalts from the Parana Plateau (Brazil): Sr-Nd isotope and geochemical evidence. *Jour. Petrol.*, **28**, 701–726.
- Rezanov, A.I., Shuto, K., Iizumi, S. and Shimura, T., 1999, Sr and Nd isotopic and geochemical characteristics of Cretaceous-Paleogene granitoid rocks in the Niigata area, the northernmost part of the Southwest Japan. *Mem. Geol. Soc. Japan*, no. 53, 269–297.
- Roberts, M.P. and Clemens, J.D., 1995, Feasibility of AFC models for the petrogenesis of calc-alkaline magma series. *Contrib. Mineral. Petrol.*, **121**, 139–147.
- Rollinson, H., 1993, *Using geochemical data: evaluation, presentation, interpretation*. Longman, Singapore, 352 p.
- Sakuyama, M., 1981, Petrological study of the Myoko and Kurohime volcanoes, Japan: crystallization sequence and evidence for magma mixing. *Jour. Petrol.*, **22**, 553–583.
- Sakuyama, M. and Nesbitt, R.W., 1986, Geochemistry of the Quaternary volcanic rocks of the Northeast Japan arc. *Jour. Volcanol. Geotherm. Res.*, **29**, 413–450.
- Shuto, K., Ohki, J., Kagami, H., Yamamoto, M., Watanabe, N., Yamamoto, K., Anzai, N. and Itaya, T., 1993, The relationships between drastic changes in Sr isotope ratios of magma source beneath the NE Japan arc and the spreading of the Japan Sea back-arc basin. *Mineral. Petrol.*, **49**, 71–90.
- Shuto, K., Tsuchiya, N., Tamura, S. and Kagami, H., 1991, Geochemistry of newly discovered Quaternary Shiribeshi volcano, Northeast Japan Sea. *Mineral. Petrol.*, **44**, 213–234.
- Shuto, K. and Yashima, R., 1990, Lateral variation of major and trace elements in the Pliocene volcanic rocks of the Northeast Japan arc. *Jour. Mineral. Petrol. Econ. Geol.*, **85**, 364–389.
- Sun, S.S. and Nesbitt, R.W., 1977, Chemical heterogeneity of Archean mantle, composition of the earth and mantle

- evolution. *Earth Planet. Sci. Lett.*, **35**, 429-448.
- Takada, A., 1994, Development of a subvolcanic structure by the interaction of liquid-filled cracks. *Jour. Volcanol. Geotherm. Res.*, **61**, 207-224.
- Takahama, N., 1976, The Neogene system in the western slope of the Asahi massif in the northern part of Niigata Prefecture, Japan. *Mem. Geol. Soc. Japan*, no. 13, 211-228.*
- Tamura, S., Kobayashi, Y. and Shuto, K., 1989, Quantitative analysis of the trace elements in silicate rocks by X-ray fluorescence method. *Earth Science (Chkyu Kagaku)*, **43**, 180-185.**
- Tsuchiya, N. and Shuto, K., 1993, Trace element chemistry of the Shiribeshi volcano, northeast Japan Sea. *Professor Jiro Ishii Memorial Volume*, 187-195.**
- Yamamoto, K., Shuto, K., Watanabe, N., Itaya, T. and Kagami, H., 1991, K-Ar ages of the Tertiary volcanic rocks from Okushiri Island and the petrological characteristics of the Oligocene to Early Miocene volcanic rocks from the Northeast Japan arc and the surrounding areas. *Jour. Mineral. Petrol. Econ. Geol.*, **86**, 507-521.*
- Yamamoto, M., 1988, Picritic primary magma and its source mantle for Oshima-Oshima and back-arc side volcanoes, Northeast Japan arc. *Contrib. Mineral. Petrol.*, **99**, 352-359.
- Yoshida, T. and Aoki, K., 1984, Geochemistry of major and trace elements in the Quaternary volcanic rocks. *Sci. Rep. Tohoku Univ.*, **III**, **16**, 1-34.
- Yoshida, T. and Aoki, K., 1988, Trace element composition of volcanic products of Oshima-Oshima volcano, Hokkaido. *Res. Rep. Lab. Nucl. Tohoku Univ.*, **21**, 268-280.**

(要 旨)

Kondo, H., Shuto, K. and Fukase, M., 2000, An AFC (assimilation and fractional crystallization) process as the petrogenesis of andesites from the Pliocene Myojin-iwa Formation, the back-arc side of the Northeast Japan: combined major- and trace-element and Sr-Nd isotope constraints. *Jour. Geol. Soc. Japan*, **106**, 426-441.

(近藤裕美・周藤賢治・深瀬雅幸, 2000, 東北日本背弧側に産する鮮新統明神岩層の安山岩類の成因—AFC プロセス—; 主要・微量元素組成および Sr・Nd 同位体組成からの制約. 地質雑, **106**, 426-441.)

東北日本の背弧側(新潟県北部)には, 鮮新世(約3Ma)の主に安山岩質の溶岩および火砕岩からなる明神岩層が分布する。これら安山岩類の斑晶鉱物組み合わせ, 斑晶鉱物の化学組成, 全岩の主要・微量元素組成などの特徴は, 安山岩の組成変化の主な要因が, 斑晶鉱物の分別にあることを示唆している。しかし, 安山岩類の SrI 値は SiO₂ 量の増加とともに高くなり, NdI 値は逆に SiO₂ 量の増加とともに低くなる傾向を示す。このことは, これらの安山岩類は玄武岩質マグマからの単純な分別結晶作用によって形成されたものではないことを示している。これらのことから, 明神岩層の周辺に分布する漸新世の花崗岩質岩石と先第三系堆積岩(これらは新潟地域の上部地殻の主な構成岩である)の同化作用の影響について検討した。その結果, 安山岩類の化学組成および同位体組成の変化は, 玄武岩質マグマが花崗岩質岩石を同化しながら分別結晶作用したことによって説明されることが明らかにされた。